World Journal of Pediatric Surgery

Radiomic-based machine learning model for predicting the surgical risk in children with abdominal neuroblastoma

Xuan Jia , Jiawei Liang, Xiaohui Ma, Wenqi Wang, Can Lai

To cite: Jia X, Liang J, Ma X, *et al*. Radiomic-based machine learning model for predicting the surgical risk in children with abdominal neuroblastoma. *World Jnl Ped Surgery* 2023;**6**:e000531. doi:10.1136/wjps-2022-000531

Received 18 November 2022
Accepted 27 March 2023

Department of Radiology, Children's Hospital, Zhejiang University School of Medicine, Hangzhou, China

Correspondence to
Dr Xuan Jia; 6202059@zju.edu.cn

ABSTRACT

Background Preoperative imaging assessment of surgical risk is very important for the prognosis of these children. To develop and validate a radiomics-based machine learning model based on the analysis of radiomics features to predict surgical risk in children with abdominal neuroblastoma (NB).

Methods A retrospective study was conducted from April 2019 to March 2021 among 74 children with abdominal NB. A total of 1874 radiomic features in MR images were extracted from each patient. Support vector machines (SVMs) were used to establish the model. Eighty percent of the data were used as the training set to optimize the model, and 20% of the data were used to validate its accuracy, sensitivity, specificity and area under the curve (AUC) to verify its effectiveness.

Results Among the 74 children with abdominal NB, 55 (65%) had surgical risk and 19 (35%) had no surgical risk. A t test and Lasso identified that 28 radiomic features were associated with surgical risk. After developing an SVM-based model using these features, predictions were made about whether children with abdominal NB had surgical risk. The model achieved an AUC of 0.94 (a sensitivity of 0.83 and a specificity of 0.80) with 0.890 accuracy in the training set and an AUC of 0.81 (a sensitivity of 0.73 and a specificity of 0.82) with 0.838 accuracy in the test set.

Conclusions Radiomics and machine learning can be used to predict the surgical risk in children with abdominal NB. The model based on 28 radiomic features established by SVM showed good diagnostic efficiency.

WHAT IS ALREADY KNOWN ON THIS TOPIC

⇒ Neuroblastoma (NB) is one of the most common solid abdominal malignant tumors in children and seriously that threatens children's lives and health.

⇒ Current therapeutic approaches for NB include surgery, chemotherapy, and radiotherapy combined with comprehensive treatment, which improve the prognosis for patients. However, surgery is still an important part of the treatment of NB, and its safety cannot be ignored.

⇒ To strive for total resection of the lesion or minimize tumor load during surgery and enable surgeons to choose a more appropriate surgical method before surgery and prevent intraoperative complications in advance, preoperative evaluation of surgical risk is of great significance to children with NB.

WHAT THIS STUDY ADDS

⇒ With the advent of the era of artificial intelligence and big data, radiomics, as an emerging technique, has been increasingly proved to have clinical significance.

⇒ Radiomics can capture automated quantitative analysis of phenotypic information through a data representation algorithm and extract meaningful imaging features from quantitative analysis of visual medical images, which can further play a role in guidance and prediction in clinical practice.

HOW THIS STUDY MIGHT AFFECT RESEARCH, PRACTICE OR POLICY

⇒ If radiomic features are combined with other clinical data of children, advanced bioinformatics tools are used to conduct in-depth excavation and develop models, and comprehensive evaluation of tumor characteristics can be carried out to improve the accuracy of preoperative evaluation.

⇒ Radiomics can realize the noninvasive, quantitative, automatic assessment of the potential of spatial heterogeneity of tumors and predict the risk.

INTRODUCTION

Neuroblastoma (NB) is one of the most common solid abdominal malignant tumors in children. It can occur anywhere along the sympathetic nervous system, accounting for approximately 6%–10% of all tumors in children with a mortality rate of 15% and seriously threatening children's life and health.[1] Although current therapeutic approaches for NB include surgery, chemotherapy and radiotherapy combined with comprehensive treatment, which improve prognosis for patients, their effect remains poor, with a high risk of recurrence[2] due to its diverse biological behavior. However, surgery is still an important part of the treatment of NB, and its safety cannot be ignored. NB has been staged with a gradual improvement from the International Neuroblastoma Staging System (INSS) to the international neuroblastoma risk group (INRG) in recent years.[3] Abdominal NB in children is often large and easily invades surrounding tissues and blood vessels,

resulting in high surgical difficulty and risk of postsurgical complications. Therefore, preoperative imaging assessment of surgical risk is very important for the prognosis of these children.

In recent years, image-defined risk factors (IDRFs) in the International Neuroblastoma risk Classification Group (INRG) have often been used as evaluation indicators[4] to predict the risk of complications associated with tumor resection. The stratified risk assessment was carried out by preoperative imaging assessment including tumor location, whether the tumor invaded important blood vessels or organs and whether it entered the spinal canal and other indicators, which suggests that the incidence of surgical complications in IDRF-positive children was much higher than that in IDRF-negative children.[5–7] Although IDRFs currently play the main role in the evaluation of surgical risk in NB, there are subjective interpretation errors. Only semiquantitative image information can be used to evaluate the structural characteristics of tumors, and there is no distinction between low-risk, medium-risk, and high-risk NB, which lacks the information needed for personalized biology and targeted therapy. It also fails to provide the molecular and gene-level biological information needed for precision medicine.

With the advent of the era of artificial intelligence and big data, radiomics, as an emerging technique, has been increasingly proved to have clinical significance. It can capture automated quantitative analysis of phenotypic information through a data representation algorithm and extract meaningful imaging features from quantitative analysis of visual medical images. Machine learning models for prediction can be established using these features,[8] which can further play a role in guidance and prediction in clinical practice. At present, a number of studies on adults have reported that the pathological classification and grading of tumors[9–13] and prognosis can be predicted before surgery by extracting radiomic features from medical images of abdominal malignant tumors and using machine learning for in-depth analysis. This study aimed to develop and validate a radiomics-based machine learning model based on the analysis of radiomics features to predict surgical risk in children with abdominal NB.

MATERIALS AND METHODS

Study population

A retrospective study was conducted from April 2019 to March 2021 among 74 children with abdominal NB at the Children's Hospital, Zhejiang University School of Medicine. Inclusion criteria included (1) patients who underwent magnetic resonance imaging (MRI) plain scan of abdomen before treatment; (2) patients whose NB was removed; (3) patients who were confirmed by pathology; and (4) patients who did not receive any treatment before diagnosis. Exclusion criteria included (1) patients who had MRI contraindications; (2) patients who failed to be sedated; (3) patients with unknown pathology; and (4) patients whose MRI artifacts were obvious.

Data collection

Patient demographic and clinical data related to NB were extracted, including age, sex, neuron-specific enolase, INSS, MCYN amplification, absence of 11q-23 and SRD-1p36 and Ki67, and distant metastasis.

Criteria for surgical risk

According to the INSS and INRG,[3] the included patients were divided into two groups: patients with surgical risk and patients without surgical risk. Criteria for surgical risk included: (1) NB surrounding peripheral large vessels (including celiac axis, superior mesenteric artery, iliac vessels and inferior vena cava); (2) NB crossing the midline; (3) NB extending into the adjacent spinal canal; (4) NB associated with lymph node metastasis (including retroperitoneal lymph nodes, mesenteric lymphoid nodes, inguinal lymph nodes, iliac vessels peripheral lymph nodes);[5] (5) NB invading one or both renal pedicles; and (6) NB invading nearby organs (including liver, pancreas, duodenum, septum).

Fifty-five patients had surgical risk, and 19 had no surgical risk among the 74 included children with abdominal NB.

Examination method

All patients were scanned on a 3.0 T MRI scanner (Achieva 3.0 T Rex, Philips) with gradient field intensity 80 mT/m, slew rate 200 mT/(m s), using a dual-channel volume coil for transmission and an eight-channel coil with high sensitivity for reception. Children under 5 years of age should be given 10% chloral hydrate for sedation by coloclysis or oral administration approximately 40 min before examination and scanned after sleep. Children were provided hearing protectors for scans under free-breathing conditions. The following sequences were used: T1-weighted (T1W), T2-weighted (T2W), fluid-attenuated inversion recovery, mix, and B1. A complete MR examination lasted 15 min. Images were retrieved from The Picture Archiving and Communication System (PACS) for imaging feature extraction.

Image processing

The 3.0 T MRI plain scan data were downloaded from PACS to a personal laptop. Two radiologists with more than 15 years of clinical experience worked together to delineate ROIs on abdominal NB images in a double-blind manner using semiautomatic image segmentation method under three-dimensional Slicer (3D Slicer).[14] Interobserver repeatability in feature delineation was preliminarily analyzed. Then, the two repeated delineations were performed according to the same procedure within 2 weeks to verify the intraobserver repeatability. The intraclass correlation coefficient (ICC) was used to determine intraobserver and interobserver differences.

Imaging feature extraction

Pyradiomics, an open-source Python package, was used to analyze and extract the radiomic features of ROIs in MR images of children with abdominal NB.[15] After undergoing

N4 bias field correction, isotropic voxel resampling and signal intensity normalization, the MR images used for radiomic feature extraction were transformed by Wavelet, Laplacian of Gaussian (LoG), Square, SquareRoot, Logarithm, and Exponential. All obtained images were extracted for radiomic features, and a total of 1874 features were obtained.

The extraction contents included first order statistics, Shape-based 3D, gray level co-occurrence matrix (GLCM), gray level run length matrix, gray level size zone matrix (GLSZM), neighboring gray tone difference matrix (NGTDM), and gray level dependence matrix (GLDM).

Statistical analysis

Demographic statistics were analyzed using R language (V.4.0.0, https://www.r-project.org/). A t test was used for age analysis, and the χ^2 test was used for gender difference analysis between the two groups. Python was used to analyze the extracted radiomic data. Pandas, Numerical Python (Numpy), Scikit-learn (Sklearn), Scipy, seaborn, and matplotlib were used for data analysis and visualization. Feature selection was performed by independent sample t test and least absolute shrinkage and selection operator (Lasso).[16] The selected radiomic features were used to establish an SVM-based model in the training set to predict the surgical risk in children with abdominal NB. After data imbalance correction via the synthetic minority oversampling technique, the prediction model was validated in the test set. The receiver operating characteristic (ROC) curve was plotted, and the area under the curve (AUC) was calculated to evaluate the performance of the model. P<0.05 was considered statistically significant. The flow chart of image processing, radiomic feature extraction and machine learning is shown in figure 1.

RESULTS

Clinical parameters

A total of 74 children with abdominal NB were included in this study, including in the training set with surgical risk and 19 in the test set without surgical risk. The mean age of patients was 4 years (0.1–13.9 years) and 4.2 years (0.2–12.1 years) in the training and test group, respectively. The results of the clinical parameters are shown in table 1.

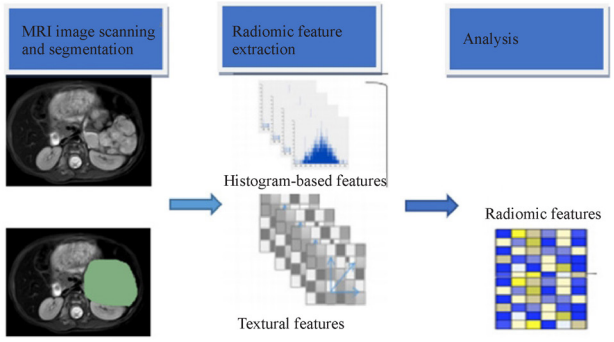

Figure 1 Flow chart of image processing, radiomic features extraction, and machine learning. MRI, magnetic resonance imaging.

Intraobserver and interobserver agreement

After the features of ROIs obtained by two radiologists underwent the ICC test, the features with poor agreement were deleted, and 1538 features with agreement above 0.75 were retained.

Radiomic feature extraction

A total of 1874 radiomic features were extracted from each patient's MRI images and filter-transformed images using pyradiomics. A t test combined with Lasso identified that 28 radiomic features were associated with surgical risk, including 11 GLCM features, 3 NGTDM features, 4 GIRIM features, 4 GLSZM features, and 3 GLDM features (table 2, figures 2 and 3). These features were significantly different between the group with surgical risk and the group with no surgical risk (p<0.05), with a weight shown in figure 4. A correlation heatmap was also drawn with the feature to evaluate collinearity and redundancy among extracted radiomic features (figure 5).

ROC analysis

Eighty percent of the included children with abdominal NB were randomly selected as the training set, and the remaining 20% were selected as the test set. An SVM-based model to predict the surgical risk in children with abdominal NB was developed by applying the radiomic features selected in the training set and then verified in the remaining test set.

Repetitive parameter optimization of SVM was performed for the best classification effect and avoided overfitting, achieving an AUC of 0.94 (a sensitivity of 0.83 and a specificity of 0.80) with 0.890 accuracy in the training set and an AUC of 0.81 (a sensitivity of 0.73 and a specificity of 0.82) with 0.838 accuracy in the test set when penalty parameter C was 100 and Gamma was 0.01 (figures 6 and 7).

DISCUSSION

NB is an embryonal malignant tumor of the sympathetic nervous system in children, and its prognosis varies greatly among children. According to the current international treatment guidelines, there is no surgical risk for NB with clear boundaries with surrounding tissues, so tumor resection can be performed directly without induction chemotherapy. However, it is considered that there is surgical risk for NB with close association with surrounding tissues; therefore, surgery can be considered only after biopsy, induction chemotherapy, and reevaluation. To strive for total resection of the lesion or minimize tumor load during surgery and enable surgeons to choose

Table 1 Demographic and clinical data of included children with abdominal NB

Variables	Missing	Overall (N=74)	Surgical risk		P value
			No (n=19)	Yes (n=55)	
Age, Mean±SD	0	4.0 (2.7)	4.2 (3.8)	4.0 (2.2)	0.774
Sex, n (%)					1.000
Female		39 (52.7)	10 (52.6)	29 (52.7)	
Male	0	35 (47.3)	9 (47.4)	26 (47.3)	
Mode, n (%)					<0.001
Yes	0	28 (37.8)	18 (94.7)	10 (18.2)	
No		46 (62.2)	1 (5.3)	45 (81.8)	
Metastasis, n (%)					
No	0	37 (50.0)	19 (100.0)	18 (32.7)	
Yes		37 (50.0)	0 (0.0)	37 (67.3)	
NSE, n (%)	1	48.0 (66.1)	28.3 (31.3)	54.4 (73.1)	0.038
I	0	11 (14.9)	10 (52.6)	1 (1.8)	
II		30 (40.5)	6 (31.6)	24 (43.6)	
INSS stage, n (%)					
III		8 (10.8)	0 (0.0)	8 (14.5)	
IV		25 (33.8)	3 (15.8)	22 (40.0)	
MCYN, n (%)					0.563
Amplification	21	49 (92.5)	14 (100.0)	35 (89.7)	
No amplification		4 (7.5)	0 (0.0)	4 (10.3)	
11q-23, n (%)					0.282
No absence	21	49 (92.5)	12 (85.7)	37 (94.9)	
Absence		4 (7.5)	2 (14.3)	2 (5.1)	
SRD-1p36, n (%)					1
No absence	21	40 (75.5)	11 (78.6)	29 (74.4)	
Absence		13 (24.5)	3 (21.4)	10 (25.6)	
Ki67, Mean±SD	1	0.2 (0.3)	0.1 (0.2)	0.2 (0.3)	0.055
NB surrounding peripheral large vessels, n (%)					< 0.001
No	0	39 (52.7)	19 (100.0)	20 (36.4)	
Yes		35 (47.3)	0 (0.0)	35 (63.6)	
NB extending into intervertebral space, n (%)					0.18
No	0	67 (90.5)	19 (100.0)	48 (87.3)	
Yes		7 (9.5)	0 (0.0)	7 (12.7)	
NB invading kidney, n (%)					0.017
No	0	61 (82.4)	19 (100.0)	42 (76.4)	
Yes		13 (17.6)	0 (0.0)	13 (23.6)	
NB crossing the midline, n (%)					0.003
No	0	52 (70.3)	19 (100.0)	33 (60.0)	
Yes		22 (29.7)	0 (0.0)	22 (40.0)	

INSS, International Neuroblastoma Staging System; MYCN, v-myc avian myelocytomatosis viral oncogene neuroblastoma derived homolog; NB, neuroblastoma; NSE, neuron-specific enolase; SD, standard deviation.

a more appropriate surgical method before surgery and prevent intraoperative complications in advance, preoperative evaluation of surgical risk is of great significance to children with NB.[17–20]

Although the rapid development of radiomic equipment and technology in recent years has allowed tumor growth and invasion to be determined according to the characteristics of morphology, density, edge, and other

Table 2 Selected radiomic features and their weights

Filter	Content	Feature	Weight
Wavelet-LLH	NGTDM	Contrast	c
Wavelet-LHL	GLCM	MCC	−0.017279351
Wavelet-LHH	GLCM	Cluster shade	0.092164975
Wavelet-LHH	GLCM	Correlation	0.006937257
Wavelet-HLL	First Order	Skewness	−0.045636121
Wavelet-HLL	GLCM	Joint energy	−0.000468081
Wavelet-HLL	GLCM	MCC	−0.003898945
Wavelet-HLL	NGTDM	Strength	−0.093386704
Wavelet-HLH	GLCM	Imc1	−0.098968757
Wavelet-HLH	GLCM	Maximum probability	0.011684371
Wavelet-HLH	GLRLM	Run entropy	0.1127218
Wavelet-HHL	First Order	Kurtosis	0.078565624
Wavelet-LLL	GLCM	Imc2	−0.04851471
Log-sigma-0–5 mm-3D	First Order	Kurtosis	−0.061965144
Log-sigma-1–0 mm-3D	GLCM	MCC	−0.023173336
Log-sigma-2–0 mm-3D	GLSZM	Large area low gray level emphasis	−0.167740327
Log-sigma-3–0 mm-3D	GLCM	Imc2	0.068711955
Log-sigma-4–0 mm-3D	GLSZM	Large area high gray level emphasis	−0.003414446
Lbp-2D	GLSZM	Size zone nonuniformity normalized	−0.001849751
Square root	GLSZM	Gray level nonuniformity normalized	0.097057736
Square root	NGTDM	Strength	−0.022030986
Logarithm	GLCM	Imc2	−0.062773043
Logarithm	GLRLM	Run entropy	−0.025857206
Logarithm	GLRLM	Run variance	−0.002688257
Exponential	First Order	Uniformity	0.077259714
Exponential	GLDM	Dependence nonuniformity normalized	0.058133675
Exponential	GLDM	Large dependence high gray level emphasis	−0.051759668
Gradient	GLDM	Small dependence low gray level emphasis	−0.030119555

First order, such as the mean, maximum, minimum, and so on.
'L' means a low-pass filter.
'H' means a high-pass filter.
'HLH', respectively, means x, y. and z axis of the wavelet filter.
'Wavelet-HLH' means that a high-pass filter, a low-pass filter and a high-pass filter was applied on x, y, and z axis of the wavelet filter, which was named analogously for 'Wavelet-HHH' and 'Wavelet-LLL'.
GLCM, gray level co-occurrence matrix; GLDM, gray level dependence matrix; GLRLM, gray level run length matrix; GLSZM, gray level size zone matrix; MCC, maximal correlation coefficient; NGTDM, neighboring gray tone difference matrix.

features, it is still difficult for radiomic doctors to quantitatively judge the local invasion of the tumor by naked eye and find a few blood vessels and lymph nodes. Although these images reveal far more valuable information than human beings can recognize, it is still difficult to effectively use them during image interpretation in practical work. Radiomics, as an in-depth medical image analysis tool, is capable of high-throughput, automated analysis, and extraction of large quantitative image features and thus has the potential to assess the spatial heterogeneity of tumors and can be used as a noninvasive tool for 'multiple virtual biopsies'.[21 22] If radiomic features are combined with other clinical data of children, advanced bioinformatics tools are used to conduct in-depth excavation and develop models, and comprehensive evaluation of tumor characteristics can be carried out to improve the accuracy of preoperative evaluation and prediction of prognosis.[23] Gao *et al*[13] used pyradiomics to conduct radiomic analysis on CT images of 165 gastric cancer patients in three independent cohorts, obtaining six robust radiomic features and established models to verify and test the good estimation of tumor infiltrating regulatory T cells (TITreg) in the cohorts. Multivariate Cox regression

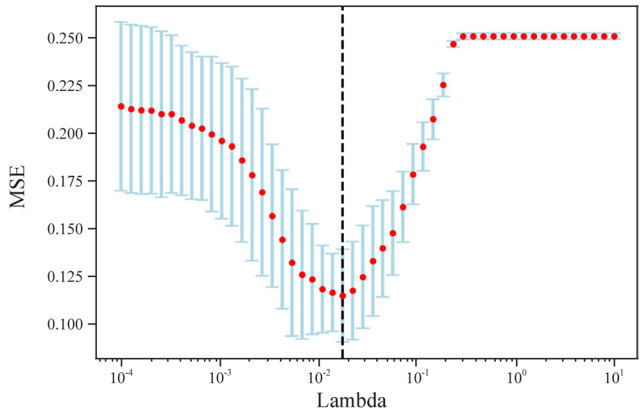

Figure 2 Lambda selection in Lasso. MSE, mean square error.

analysis showed that the radiomic feature was an independent risk factor for poor overall survival in patients with gastric cancer. Kaissis *et al*[24] applied pyradiomics to analyze preoperative CT images of 207 patients with pancreatic duct adenocarcinoma and developed a random forest machine learning algorithm to predict molecular subtypes of pancreatic cancer based on radiomic features. The sensitivity, specificity, and AUC were 0.84±0.05, 0.92±0.01, and 0.93±0.01, respectively, suggesting that radiomics analysis could predict the molecular subtypes highly correlated with the survival of patients with pancreatic cancer.

In our study, pyradiomics was used to achieve radiomic feature extraction, and a t test and Lasso were used to identify 28 radiomic features associated with surgical risk from a large number of radiomic features. These radiomic features showed statistical features between NB cohorts with and without surgical risk. The SVM-based prediction model achieved an AUC of 0.94 (a sensitivity of 0.83 and a specificity of 0.80) with 0.890 accuracy in the training set and an AUC of 0.81 (a sensitivity of 0.73 and a specificity of 0.82) with 0.838 accuracy in the test set, showing a good effect. This result indicated that radiomics and machine learning were feasible for predicting the surgical risk in children with abdominal NB. The

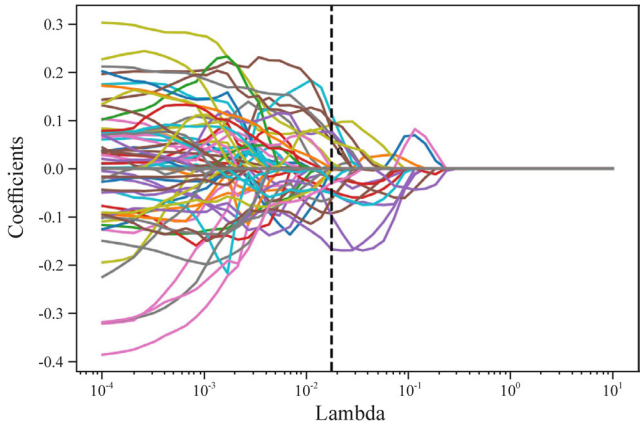

Figure 3 Curve of coefficient with Lambda changes when using Lasso selecting radiomic features.

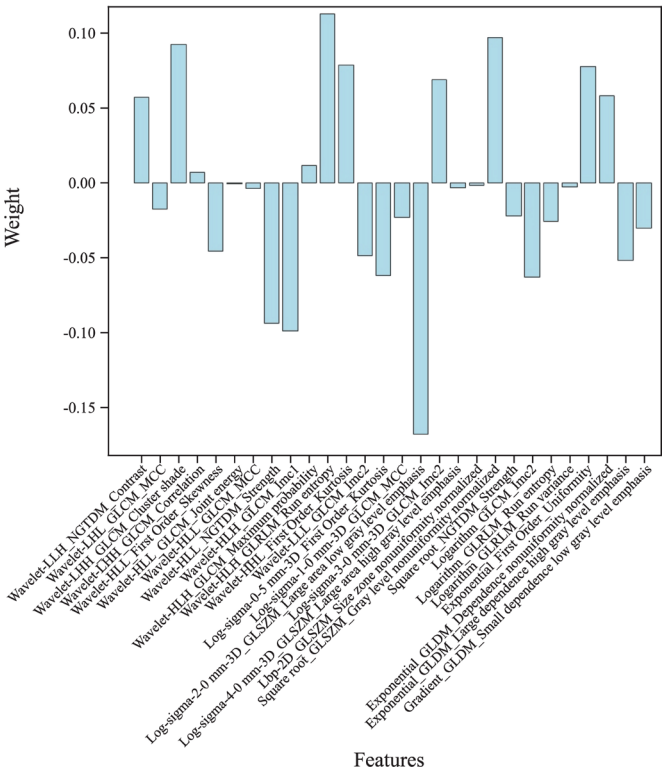

Figure 4 Weights of radiomic features obtained by selecting. ('L' means a low-passfilter. 'H' means a high-passfilter. 'HLH', respectively, means x, y. and z axis of the wavelet filter. 'Wavelet-HLH'means that a high-passfilter, a low-passfilter and a high-passfilter was applied on x, y, and z axis of the wavelet filter, which was named analogously for 'Wavelet-HHH'and 'Wavelet-LLL'). GLCM, gray level co-occurrencematrix; GLDM, gray level dependence matrix; GLRLM, gray level run length matrix; GLSZM, gray level sizezone matrix; MCC, maximal correlation coefficient; NGTDM, neighboring gray tone difference matrix.

GLCM and GLSZM in the model based on 28 radiomic features established by SVM had greater weights. Considering the relatively small number of children included in the analysis, we believe that the classification of 28 radiomic features in these six categories for surgical risk in NB should be interpreted carefully. At present, it is only a preliminary exploration.

There were some limitations in our study:[1] Due to the limitation of the number of patients, the sample size for machine learning is still relatively small. After expanding the sample size in the future, more parameters can be included for modeling to observe whether the prediction ability of the model can be further improved.[2] This study lacked an independent validation set. To ensure that our method can be extended to independent data, further research and validation in independent data sets are needed. We plan to seek multicenter cooperation to remedy this defect.[3] Parmar *et al*,[25] through in-depth studies, believed that the selection of classification methods was the most important factor for performance differences (accounting for 34.21% of the total differences), and the determination and application of

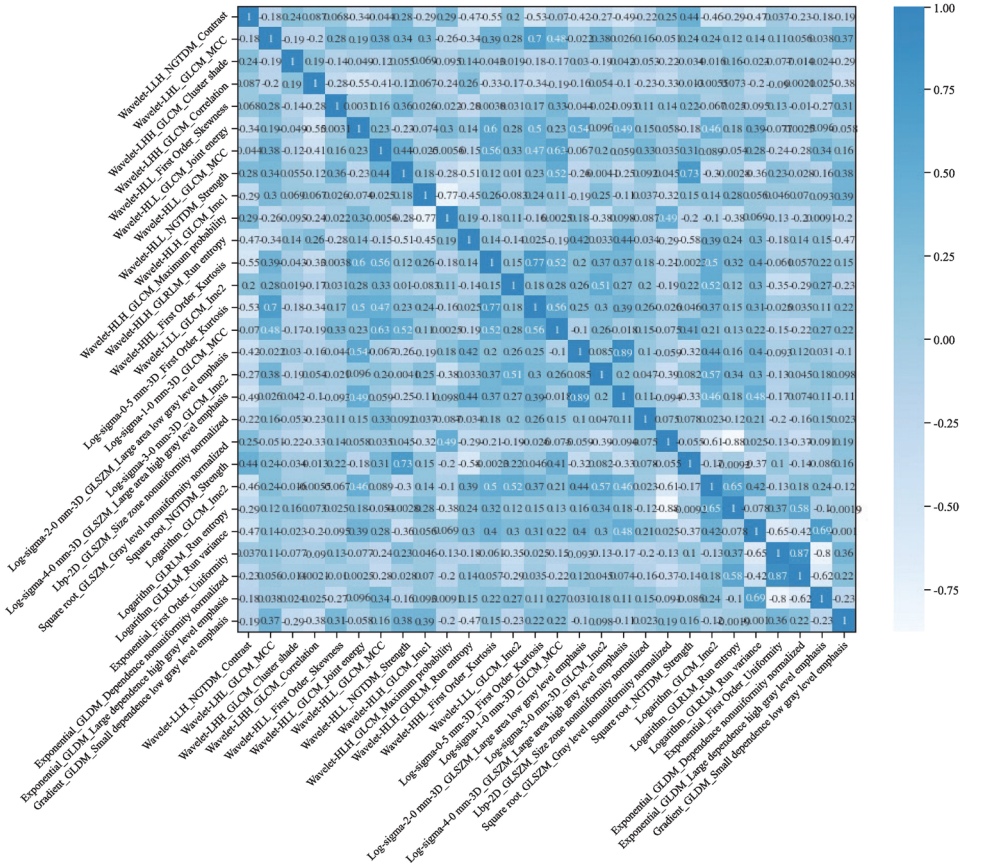

Figure 5 A correlation heatmap of radiomic feature ('L' means a low-passfilter. 'H' means a high-passfilter. 'HLH', respectively, means x, y. and z axis of the wavelet filter. 'Wavelet-HLH'means that a high-passfilter, a low-passfilter and a high-passfilter was applied on x, y, and z axis of the wavelet filter, which was named analogously for 'Wavelet-HHH'and 'Wavelet-LLL'). GLCM, gray level co-occurrencematrix; GLDM, gray level dependence matrix; GLRLM, gray level run length matrix; GLSZM, gray level sizezone matrix; MCC, maximal correlation coefficient; NGTDM, neighboring gray tone difference matrix.

the best machine learning method was an important step to explore stable and clinically relevant radiomic biomarkers. In this study, we only verified SVM machine learning to develop a radiomic model. Whether other classifiers have better effects was not involved. We will further explore and verify the effectiveness of other classifiers in future studies.

In summary, this study attempted to predict surgical risk in children with abdominal NB via radiomics and machine learning. SVM was used to establish a machine learning model based on 28 radiomic features. The results showed that the model had a high accuracy in distinguishing preoperative surgical risk for abdominal

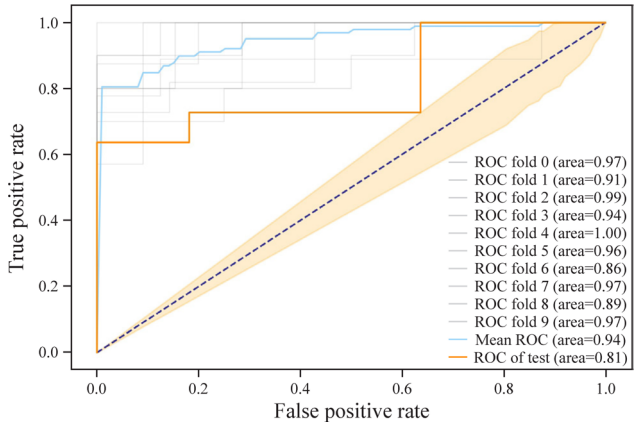

Figure 6 ROC curve of SVM-based model to predict the surgical risk in abdominal NB. NB, neuroblastoma; ROC, receiver operating characteristic; SVM, support vector machines.

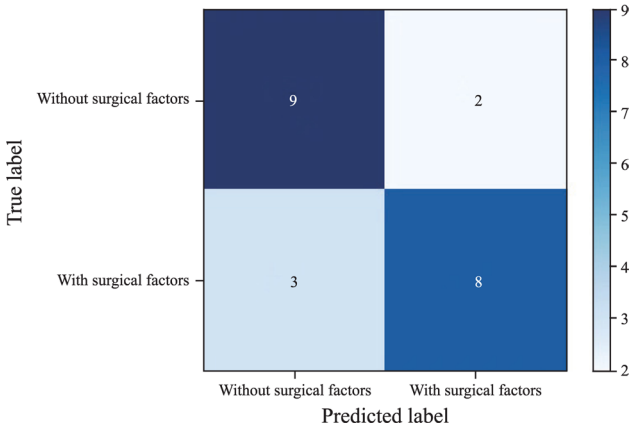

Figure 7 Matrix diagram of test set classification.

NB, which could provide a reference for the quantitative selection of clinical treatment strategies.

Contributors XJ contributed to manuscript preparation and data collection. JL and XM contributed to manuscript preparation. WW and CL contributed to manuscript editing and review. XJ is responsible for the overall content as guarantor. She accepts full responsibility for the finished work and/or the conduct of the study, had access to the data, and controlled the decision to publish.

Funding The authors have not declared a specific grant for this research from any funding agency in the public, commercial or not-for-profit sectors.

Competing interests None declared.

Patient consent for publication Not applicable.

Ethics approval This study involves human participants and was approved by The Ethics Committee of the Children's Hospital Affiliated to Zhejiang University School of Medicine, and all guardians of the subjects understood the contents of the examination before conduction and signed the informed consent form (2021-IRB-117). Participants gave informed consent to participate in the study before taking part.

Provenance and peer review Not commissioned; externally peer reviewed.

Data availability statement Data sharing not applicable as no datasets generated and/or analyzed for this study. No data are available.

ORCID iD

Xuan Jia http://orcid.org/0000-0002-5810-3390

REFERENCES

1 He WG, Ren G, Cai R, *et al*. The value of CT in diagnosis and differential diagnosis of abdominal neuroblastoma and ganglioneuroblastoma in children. *Radiologic Practice* 2018;33:493–7.
2 Zhao SZ. Diagnostic value of CT and MRI in neuroblastoma of central nervous system. *Journal of Imaging Research and Medical Applications* 2018;2:140–1.
3 Hu JJ, Sun JH, Chen YW, *et al*. Correlational research between image danger risk factor and surgical complications of retroperitoneal neuroblastoma in children. *Journal of Clinical Pediatric Surgery* 2020;19:903–8.
4 Cecchetto G, Mosseri V, De Bernardi B, *et al*. Surgical risk factors in primary surgery for localized neuroblastoma: the LNESG1 study of the European International Society of pediatric oncology neuroblastoma group. *J Clin Oncol* 2005;23:8483–9.
5 Monclair T, Mosseri V, Cecchetto G, *et al*. Influence of image-defined risk factors on the outcome of patients with localised neuroblastoma. A report from the LNESG1 study of the European International Society of paediatric oncology neuroblastoma group. *Pediatr Blood Cancer* 2015;62:1536–42.
6 Varan A, Kesik V, Şenocak ME, *et al*. The efficacy of delayed surgery in children with high-risk neuroblastoma. *J Cancer Res Ther* 2015;11:268–71.
7 Irtan S, Brisse HJ, Minard-Colin V, *et al*. Image-defined risk factor assessment of neurogenic tumors after neoadjuvant chemotherapy is useful for predicting intra-operative risk factors and the completeness of resection. *Pediatr Blood Cancer* 2015;62:1543–9.
8 Lambin P, Rios-Velazquez E, Leijenaar R, *et al*. Radiomics: extracting more information from medical images using advanced feature analysis. *Eur J Cancer* 2012;48:441–6.
9 Nougaret S, Vargas HA, Lakhman Y, *et al*. Intravoxel incoherent motion-derived histogram metrics for assessment of response after combined chemotherapy and radiation therapy in rectal cancer: initial experience and comparison between single-section and volumetric analyses. *Radiology* 2016;280:446–54.
10 Kan Y, Dong D, Zhang Y, *et al*. Radiomic signature as a predictive factor for lymph node metastasis in early-stage cervical cancer. *J Magn Reson Imaging* 2019;49:304–10.
11 Giganti F, Antunes S, Salerno A, *et al*. Gastric cancer: texture analysis from multidetector computed tomography as a potential preoperative prognostic biomarker. *Eur Radiol* 2017;27:1831–9.
12 Kaissis GA, Ziegelmayer S, Lohöfer FK, *et al*. Image-Based molecular phenotyping of pancreatic ductal adenocarcinoma. *J Clin Med* 2020;9:724.
13 Gao X, Ma T, Bai S, *et al*. A CT-based radiomics signature for evaluating tumor infiltrating Treg cells and outcome prediction of gastric cancer. *Ann Transl Med* 2020;8:469.
14 Jolesz FA. *Intraoperative imaging and image-guided therapy*. New York: Springer, 2014: 277–89.
15 van Griethuysen JJM, Fedorov A, Parmar C, *et al*. Computational radiomics system to decode the radiographic phenotype. *Cancer Res* 2017;77:e104–7.
16 Vasquez MM, Hu C, Roe DJ, *et al*. Least absolute shrinkage and selection operator type methods for the identification of serum biomarkers of overweight and obesity: simulation and application. *BMC Med Res Methodol* 2016;16:154.
17 Tustison NJ, Avants BB, Cook PA, *et al*. N4ITK: improved N3 bias correction. *IEEE Trans Med Imaging* 2010;29:1310–20.
18 Shinohara RT, Sweeney EM, Goldsmith J, *et al*. Statistical normalization techniques for magnetic resonance imaging. *Neuroimage Clin* 2014;6:9–19.
19 Simon T, Hero B, Schulte JH, *et al*. 2017 GPOH guidelines for diagnosis and treatment of patients with neuroblastic tumors. *Klin Padiatr* 2017;229:147–67.
20 Chen J, Jiang B, Jun Y, *et al*. Application of image-defined risk factors for assessing operative risks of thoracoabdominal localized neuroblastoma. *Chinese Journal of Pediatric Surgery* 2019;40:678–82.
21 Wang HM. Techniques and principles of surgical treatment of neuroblastoma. *Journal of China Pediatric Blood and Cancer* 2014;19:7–9.
22 Trebeschi S, Drago SG, Birkbak NJ, *et al*. Predicting response to cancer immunotherapy using noninvasive radiomic biomarkers. *Ann Oncol* 2019;30:998–1004.
23 Gillies RJ, Kinahan PE, Hricak H. Radiomics: images are more than pictures, they are data. *Radiology* 2016;278:563–77.
24 Kaissis GA, Ziegelmayer S, Lohöfer FK, *et al*. Image-based molecular phenotyping of pancreatic ductal adenocarcinoma. *J Clin Med* 2020;9:724–33.
25 Parmar C, Grossmann P, Bussink J, *et al*. Machine learning methods for quantitative radiomic biomarkers. *Sci Rep* 2015;5:13087.